







## INFLUENCE OF SPECIFIC WEIGHT AND WALL FRICTION COEFFICIENT ON NORMAL PRESSURES IN SILOS USING THE FINITE ELEMENT METHOD

Rômulo Marçal Gandia\*<sup>1</sup> , Francisco Carlos Gomes<sup>1</sup> , Wisner Coimbra de Paula<sup>2</sup>  & Pedro José Aguado Rodriguez<sup>3</sup> 

1 - Federal University of Lavras, Department of Agricultural Engineering, Lavras, Minas Gerais, Brazil

2 - Federal University of Lavras, Department of Engineering, Lavras, Minas Gerais, Brazil

3 - University of León, School of Agricultural and Forestry Engineering, León, Castilla y León, Spain

### Keywords:

Jenike shear test  
Maximum normal pressures  
Numerical model  
Properties of stored products  
Simulation

### ABSTRACT

The objective of this work was to develop models using the Finite Element Method (FEM) to assess the maximum normal pressures in the static condition in silos using different wall friction coefficient and specific weight of the stored product compared to the pressures obtained by the Eurocode 1, part 4. The geometries of the silos models were developed based on the dimensions of the experimental station at the Universidad de Leon (Spain). The material properties were obtained by Jenike shear cell tests and were used to generate the models by the MEF. 3D models were generated varying the friction coefficient (0.2, 0.4, and 0.6) and the specific weight (6; 7.5 and 9 KN m<sup>-3</sup>). It was verified that the models by FEM follow the theory of pressures in silos: normal pressures increase due to the increase in specific weight and decrease due to the increase in the friction coefficient. Moreover, the maximum normal pressure occurs at the hopper silo transition. The experimental pressures (FEM models) compared with Eurocode 1, part 4 allowed to validate the models developed, presenting trends of similar values to those found by the MEF. The experimental models demonstrated that the influence of the wall friction coefficient and specific weight significantly interferes with the pressures in slender silos.

### Palavras-chave:

Simulação  
Propriedades dos produtos armazenados  
Máquina de cisalhamento de Jenike  
Modelo numérico  
Pressões normais máximas

### INFLUÊNCIA DO PESO ESPECÍFICO E DO COEFICIENTE DE ATRITO DA PAREDE NAS PRESSÕES NORMAIS EM SILOS USANDO O MÉTODO DOS ELEMENTOS FINITOS

### RESUMO

O objetivo deste trabalho foi desenvolver modelos utilizando o Método dos Elementos Finitos (MEF) para avaliar as pressões máximas normais na condição estática em silos variando o peso específico e o coeficiente de atrito do produto armazenado e posterior comparação com a Eurocode 1, parte 4. Foram desenvolvidas as geometrias dos modelos dos silos baseadas nas dimensões da estação experimental da Universidad de Leon (Espanha). As propriedades dos materiais foram obtidas por ensaios da célula de cisalhamento de Jenike e foram utilizadas para geração dos modelos pelo MEF para posterior comparação com as pressões calculadas pela Eurocode. Foram gerados modelos 3D variando o coeficiente de atrito (0,2; 0,4 e 0,6) e o peso específico (6; 7,5 e 9 KN m<sup>-3</sup>). Foi verificado que os modelos correspondem ao que é esperado diante das teorias: as pressões normais aumentam em decorrência do aumento do peso específico e diminuem pelo aumento do coeficiente de atrito. Foi constatado que a pressão normal máxima ocorre na transição silo tremonha. A das pressões comparação com a Eurocode 1, parte 4 viabilizou a validação dos modelos desenvolvidos, apresentando valores próximos e inferiores ao encontrado pelo MEF. Os modelos gerados pelo MEF demonstraram que a influência do coeficiente de atrito e peso específico interfere significativamente nas pressões em silos esbeltos. Além disso, verificou a viabilidade dos modelos para obtenção das pressões normais pelo MEF, pois apresentaram comportamento semelhante a modelo experimentais e pela Eurocode.

## INTRODUCTION

In 2020, the estimated grain production in Brazil was 268.7 million tons (CONAB, 2020). In less than 39 years (2019), Brazil has more than quadrupled its static capacity (177.7 million tons of grain). Out of this total, 86.6 million tons of grain (49%) were stored in silos (DPE, 2019).

Since 1895, Janssen (JANSSEN, 1895) has been studying the flow and pressure of products stored in silos. Ever since then, other theories have been developed (WALKER, 1967) (WALTERS, 1973a, 1973b) (JENIKE *et al.*, 1973) supporting international standards (CEN, 2006; DIN, 2005). It is necessary to understand the different theories that support the standards to comprehend the actions (flow and pressures) in silos. However, many factors are still not conclusive due to the randomness of the physical properties of the stored products (differently from liquids) (CALIL; CHEUNG, 2007).

The specific weight of the main agricultural products in Brazil (corn, soybeans, rice, wheat, and beans) (CONAB, 2020) and products derived from the feed and flour industry vary widely. For example, flour can have bulk unit weight from 6.5 to 7 KN m<sup>-3</sup>, while corn and soybean from 7 to 8 KN m<sup>-3</sup> and wheat from 7.5 to 9 KN m<sup>-3</sup> (CEN, 2006). The wall friction coefficient and the specific mass of the main agricultural products grown in Brazil varies considerably and is directly influenced by the roughness of the wall of the silo. The wall friction coefficient of this stored products are: flour (0.24 to 0.48); corn (0.22 to 0.53); soybean 0.24 to 0.48 and wheat 0.24 to 0.57 (CEN, 2006).

The main reason for the several failures and collapses in silos are the design errors and overpressures (BYWALSKI; KAMIŃSKI, 2019; GUTIÉRREZ *et al.*, 2015; DOGANGUN *et al.*, 2009; SUN *et al.*, 2006; WANG, 2012; TENG *et al.*, 2001; TENG, 1994; TENG; ROTTER, 1989, 1991).

The reason for the small number of silo full-scale experimental stations in the world is the high cost of installation, handling and, instrumentation (BROWN *et al.*, 2000; COUTO *et al.*, 2012; GANDIA *et al.*, 2021; HÄRTL *et al.*, 2008; NETO; NASCIMENTO; SILVA, 2014; RAMÍREZ *et al.*, 2010; SCHURICHT *et al.*, 2001; SCHWAB *et al.*, 1994; SUN *et al.*, 2020; TENG; LIN, 2005; TENG *et al.*, 2001; ZHAO; TENG, 2004; ZHONG *et al.*,

2001). In addition, the scale factor is crucial for reliable data (scale errors) (BROWN; NIELSEN, 1998). Therefore, even though the experimental study is vital in most science, the search for other alternatives with relatively more minor costs and less time for analysis for scientific advancement is inevitable.

Due to the advancement of engineering combined with computational development, modeling is supported by a tripod: theoretical model, experimental model, and numerical model. These three models (working together) optimize and advance studies in most areas of engineering. For example, the finite element method (FEM) is a numerical procedure to determine approximate solutions of value problems on the contour of differential equations. The FEM subdivides the problem domain into smaller parts, denominated finite elements. Therefore, in recent years, studies using the FEM in silos have significantly increased (JOFRIET, 1992; HOLST *et al.*, 1999; AYUGA *et al.*, 2006; GALLEGO *et al.*, 2010; GALLEGO; RUIZ; AGUADO, 2015; PARDIKAR *et al.*, 2020; WASSGREN, 2020; ZHAO, 2004), mainly for the quality of the answers and for the relative time and cost-saving in comparison to the experimental models in real scale.

Therefore, the objective of this paper is to simulate through the Finite Element Method, the interference of the specific mass and the wall friction coefficient using representative values of the leading Brazilian agricultural products to obtain the normal static pressures in slender silos compared to the Eurocode 1, part 4 (CEN, 2006).

## MATERIAL AND METHODS

The numerical simulation was performed using elements and the software Ansys 2020R2 student version. The model was developed by simulating the static condition (after filling the silo). The dimensions of the silo, hopper inclination were based on the silo of the experimental station designed to evaluate the pressure in silos at the University of León (Spain) designed and built by the research group of the Department of Agricultural Engineering and Sciences (COUTO; RUIZ; AGUADO, 2012; RUIZ; COUTO; AGUADO, 2012).

The silo was 2.00 meters high and had one

meter in diameter with a concentric hopper angle of 34.3 and 0.48 meters in height. The silo is made of polished steel metal. According to Eurocode 1, part 4 (CEN, 2006), this silo is classified as slender (height/diameter ratio = 2) and can be seen in Figure 1.



**Figure 1.** Silo geometry (COUTO *et al.*, 2012)

For the numerical simulation, three different wall friction coefficients and the product ( $\mu$ ) were used: 0.2; 0.4, and 0.6 (values that include the limits of wall friction coefficient of most of the leading national agricultural products (corn, soybeans, rice, wheat, and beans) (CEN, 2006) and also products characterized as feed and flour. In addition, as variables, the specific weight of the stored product ( $\gamma$ ) (6; 7.5 and 9 KN m<sup>-3</sup>) was also analyzed. Those are values that include the upper and lower specific weight of most agricultural products, such as corn, wheat, soybeans, rice, beans, and flour products from the animal feed industry.

The parameters of the stored product and the steel sheet of the silo were obtained in the literature (Table 1).

The proposed model was performed using elastoplastic material (DRUCKER; PRAGER, 1952) to simulate the pressure of the stored product (solid) inside the silo. The standard isotropic and linear model was used to represent the elastic behavior of the silo, while Drucker and Prager's perfect plasticity criterion (DRUCKER; PRAGER, 1952) was used to define the plastic part.

The model was created in 3D geometry, aiming at further studies to understand the volume of the

**Table 1.** Stored product and steel parameters

Material parameter	Value	Reference
<b>stored material</b>		
Specific weight, $\gamma$ (KN m <sup>-3</sup> )	6; 7.5; 9	-
Modulus of elasticity, $E$ (kPa)	5000	GALLEGO <i>et al.</i> , 2015)
Poisson's ratio, $\nu$	0.3	GALLEGO <i>et al.</i> , 2015)
Wall friction coefficient, $\mu$	0.2; 0.4; 0.6	-
Cohesion, $c$ (kPa)	0.71	(MOYA <i>et al.</i> , 2002)
Angle of dilatancy of bulk material, $\psi_i$	2.5	(MOYA <i>et al.</i> , 2006)
Effective angle of internal friction of bulk material, $\phi_i$	25	(MOYA <i>et al.</i> , 2006)
<b>steel sheet</b>		
Modulus of elasticity, $E$ (kPa)	210000000	(GALLEGO <i>et al.</i> , 2015)
Poisson's ratio, $\nu$	0.3	(GALLEGO <i>et al.</i> , 2015) (MOYA <i>et al.</i> , 2006)
Thickness (m)	0.02	-



model. The modeling was done initially using a small number of elements (mesh simplification). After the model was defined and generated, the mesh was refined, mainly in the areas of most significant interest (silos-hopper transition) (Figure 2). The size of the elements was 0.15 m for the solid and 0.075 m for the silo, totaling 14688 elements. The generated mesh was composed of prismatic elements with 8 and 4 knots, as shown in Figure 2. This type of mesh is stable and, when possible, allows analysis with better results. For the stored product (solid), an element with eight nodes (Solid 45, Lagrangian type) was used, which is an element that supports large deformations (GALLEGO *et al.*, 2015). The silo (shell) wall was modeled using the 8-node shell element (Shell 63), ideal for analyzing non-linear applications. For the contact (friction) between the stored product (solid) and the silo wall (shell), 4-node elements were used (Conta 173 and Target 170) (GALLEGO *et al.*, 2010). The model was vertically (z-axis) constrained in the contour of the silos-hopper transition. The gravitational force was inserted towards the z-axis.

The models were subsequently compared with Eurocode 1, part 4 (CEN, 2006). The normal static pressure curves were calculated using the same parameters proposed in the development of

the model using FEM: silo dimensions (height: 2 meters; internal diameter: 1 meter;  $\beta$ : 34.3 °); work variables (wall friction coefficient: 0.2; 0.4 and 0.6); specific weight: 6; 7.5 and 9 KN m<sup>-3</sup>; other values extracted from Table E.1 - Properties of Disaggregated Solids used for the product (CEN, 2006).

## RESULTS AND DISCUSSION

Information on Z displacement (m), Z stress (KN m<sup>-2</sup>), and main stress (KN m<sup>-2</sup>) of the mass of the product inside the silo was extracted according to the variation of the wall friction coefficient (Figure 3) and a specific weight (Figure 4).

The main tension increased as the wall friction coefficient (Figure 3a) decreased. The maximum values (SMN) are negative because they are in the opposite direction to the Z-axis, which corroborates the statements (CEN, 2006; JENIKE *et al.*, 1973). It is observed that the lowest stresses (red) occur at the top of the silo and the highest (blue) near the silos-hopper transition.

The maximum stresses in Z showed the opposite behavior, increasing according to the increase of the wall friction coefficient, mainly in the silos-hopper transition. The reason is that with the increase in

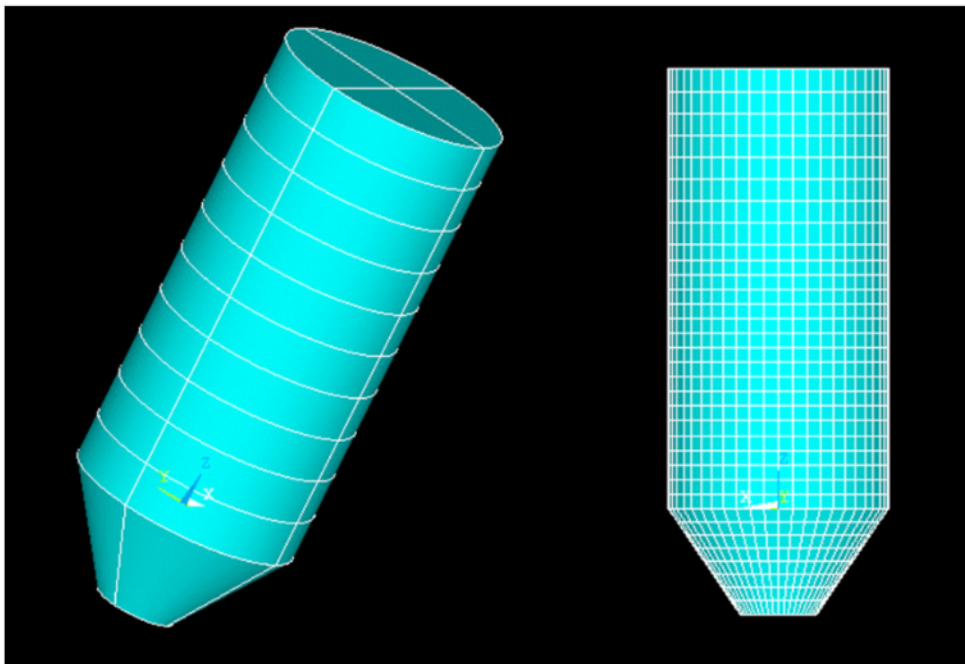


**Figure 2.** Geometry and mesh of the developed model

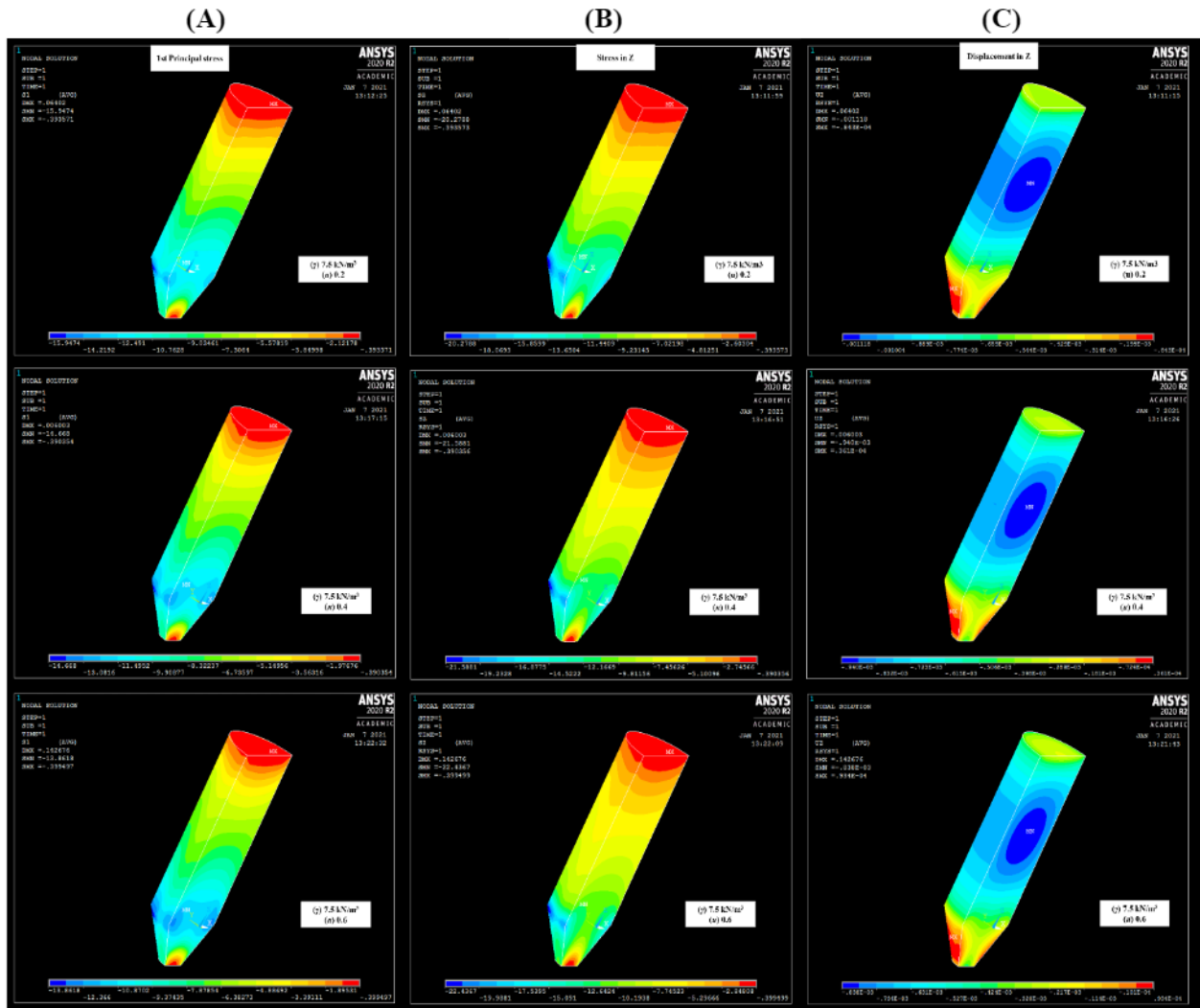


**Figure 3.** Main stress (a), stress in Z (b), and displacement in Z (c) by increasing the wall friction coefficient

the wall friction coefficient, the friction pressure increases, resulting in a reduction in the normal pressure in the silo's wall and the occurrence of a slight increase in the vertical tension in the silo-hopper transition.

A decrease was found in the displacement of the grain mass (Figure 3c) caused by the vertical displacement (z) due to the increase in the wall friction coefficient, which was visually observed through the smaller area of the ellipse (blue) approximately in the middle of the silo and numerically confirmed by the displacement value (SMN) plotted in each simulation: 1.118; 0.940 and 0.838 mm respectively for the wall friction coefficient 0.2; 0.4 and 0.6.

The main tension increased according to the increase in the specific weight of the stored product (CEN, 2006; JENIKE *et al.*, 1973) (Figure 4a). The

lowest stresses (red) occur at the top of the silo and the highest (blue) near the silo-hopper transition. However, for the specific weight of  $9 \text{ KN m}^{-3}$ , the minimum main stress occurs at the outlet gate because the increase in the specific weight of the material and the pressure of the material column above the hopper provides a mechanical arc above the outlet opening.

The maximum stresses in Z have the same dynamic, increasing according to the increase in the specific weight of the stored product, mainly in the silo-hopper transition. Thus, the maximum and minimum principal stresses occur at the hopper silo transition and the top of the silo. Except for the specific weight of  $9 \text{ KN m}^{-3}$ , where the minimum occurs at the outlet gate due to the formation of the mechanical arc provided by the increase in weight of the product, the hopper's inclination, and the wall friction coefficient of the hopper.

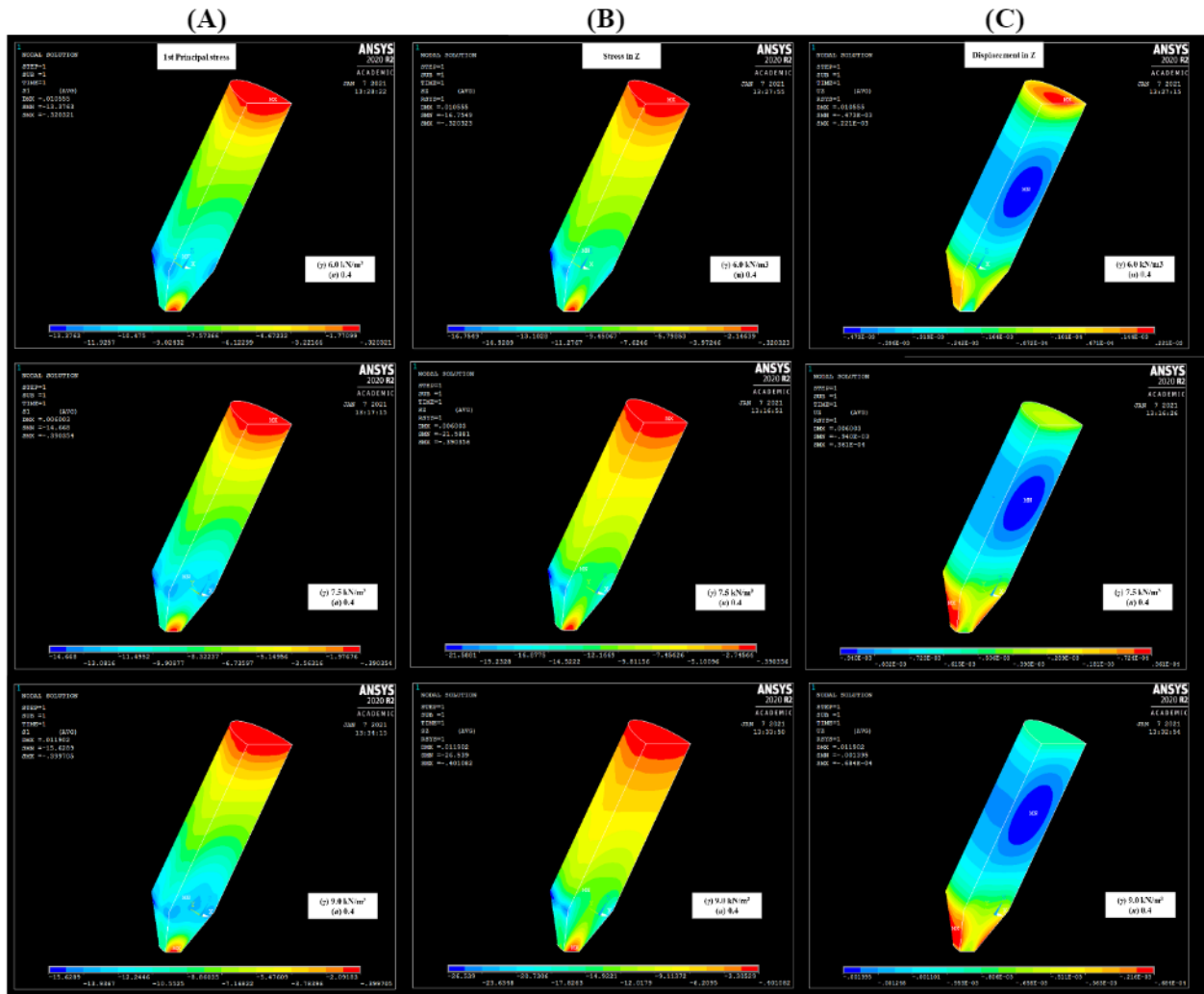


**Figure 4.** Main stress (a), stress in Z (b), and displacement in Z (c) by increasing the specific weight of the stored product

The displacement in the z (vertical) direction increased according to the specific weight of the stored material. The greater the weight of the product, the greater the displacement of the grain mass, as compression occurs according to the upper layers of the product, forcing the more significant displacement in the lower positions of the silo.

For a better comparison among the developed simulations, the normal static pressure curves were measured throughout the silo. The curves comparing the three models varying the wall friction coefficients (Figure 5) and the specific weight of the stored product (Figure 6) are shown below.

The natural behavior among the three curves varying the wall friction coefficient ( $\mu$ ) is expected

in view of the theories and experiments (CEN, 2006; INTERNACIONAL ORGANIZATION FOR STANDARDIZATION, 2012; JENIKE *et al.*, 1973; WALKER, 1967). The reason is that normal pressures have maximum values close to the hopper transition. Also, as expected in the face of theories (JENIKE; JOHANSON; CARSON, 1973; WALKER, 1967) and standards (CEN, 2006; INTERNACIONAL ORGANIZATION FOR STANDARDIZATION, 2012), the higher the wall friction coefficient, the lower the normal pressures will be due to the increased friction pressure. Therefore, the model with a wall friction coefficient ( $\mu$ ) 0.2 was the one with the highest normal pressures and 0.6 showed the lowest normal pressure values.

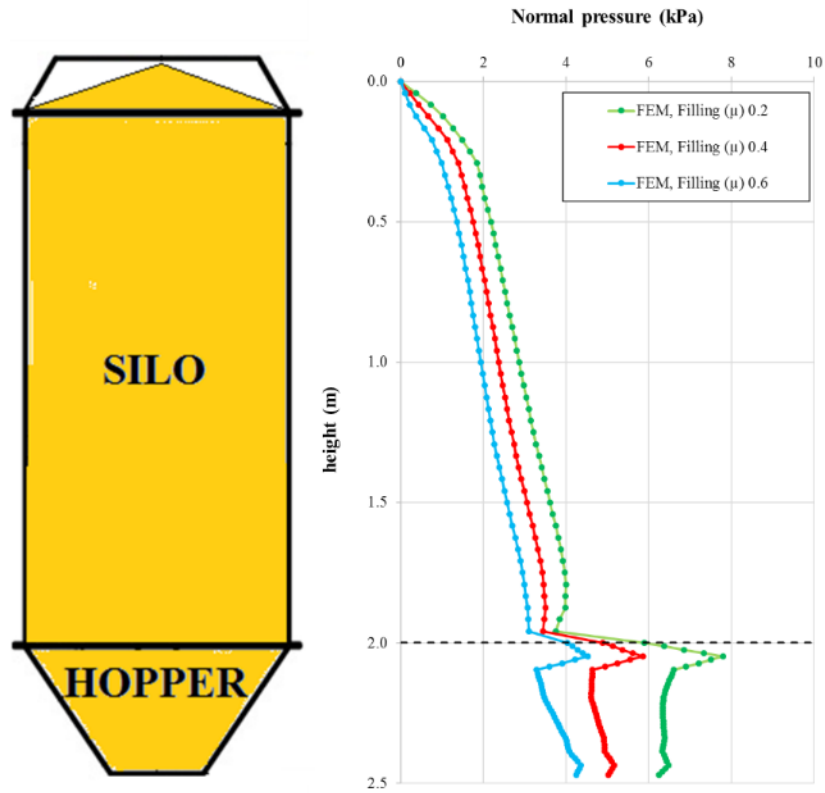


**Figure 5.** Normal static pressures varying with the wall friction coefficient

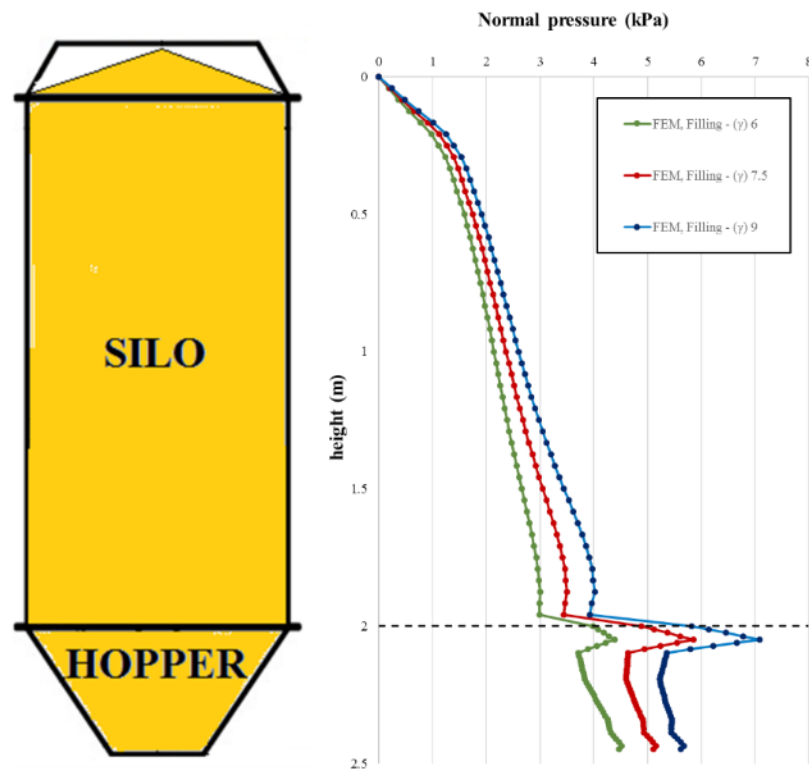


**Figure 6.** Normal static pressures varying with the specific weight of the stored product



The standard behavior among the three curves varying the specific weight of the stored product ( $\gamma$ ) was expected given the theories and codes (CEN, 2006; INTERNACIONAL ORGANIZATION FOR STANDARDIZATION, 2012; JENIKE *et al.*, 1973; WALKER, 1967). Thus, normal pressures have maximum values close to the hopper transition. Also, as expected given theories and standards, the greater the specific weight of the stored product, the greater the normal pressures on the wall and hopper. Therefore, it is observed that the model with specific weight ( $\gamma$ )  $9 \text{ KN m}^{-3}$  was the one with the highest pressure values and  $6 \text{ KN m}^{-3}$  showed the lowest values.

Aiming to validate the models and analyze Eurocode 1, part 4 (CEN, 2006), all the developed models were compared to the standard. The curves comparing the three models varying the wall friction coefficients and the pressures obtained by Eurocode 1, part 4 are shown below (Figure 7). The curves comparing the three models varying the specific weight of the stored product and the pressures obtained by Eurocode 1, part 4 are shown below (Figure 8).

The analysis of errors relating to the pressures obtained through the simulation using FEM and those calculated with Eurocode 1, part 4 was shown in Table 2.

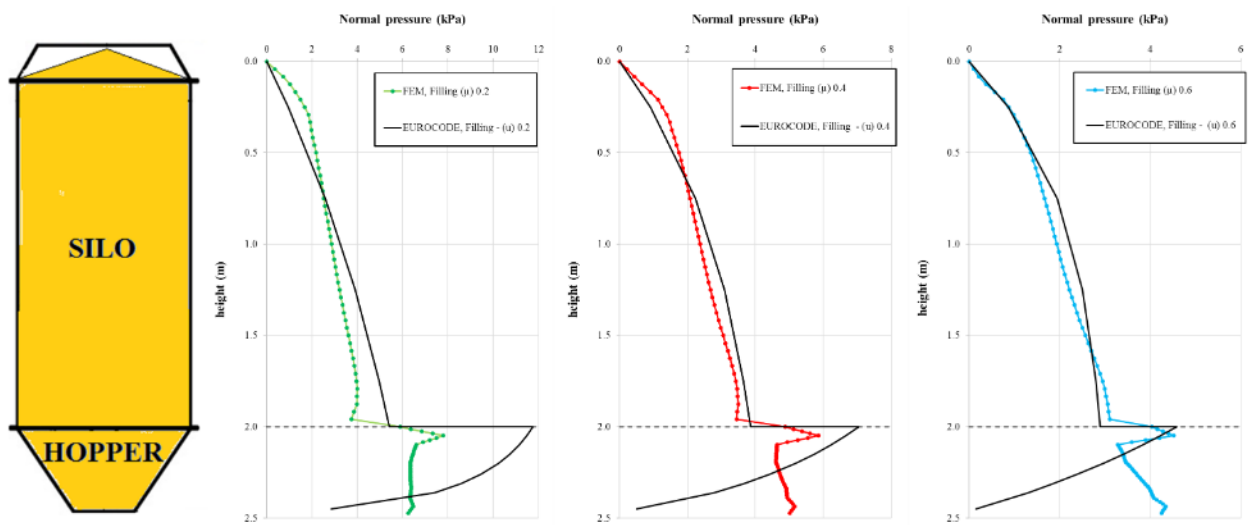


Figure 7. Normal static pressures varying the wall friction coefficient and compared with Eurocode 1, part 4

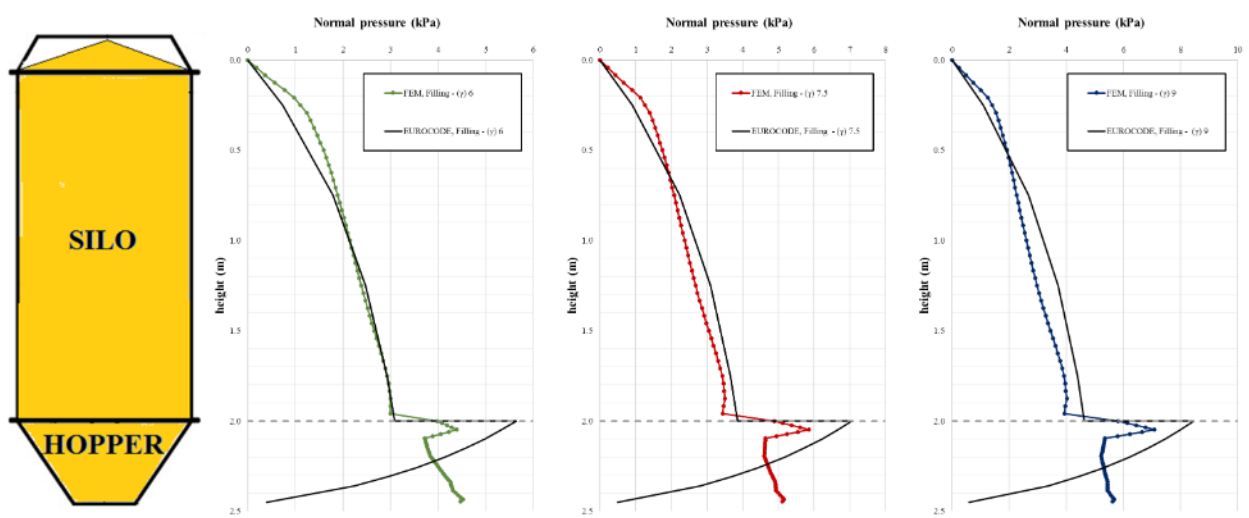


Figure 8. Normal static pressures varying the specific weight of the stored product and compared with Eurocode 1, part 4



**Table 2.** Error analysis – FEM / Eurocode1, part 4

Silo height (m)	Error (%)					
	specific weight ( $\gamma$ ) - KN m <sup>-3</sup>			wall friction coefficient ( $\mu$ )		
	6.0	7.5	9.0	0.2	0.4	0.6
0.00	0.00	0.00	0.00	0.00	0.00	0.00
0.25	34.17	27.79	21.83	42.42	27.79	0.80
0.75	5.36	-7.85	-18.51	-2.87	-7.85	-16.69
1.25	-3.85	-15.57	-24.83	-21.73	-15.57	-13.10
1.75	0.13	-6.79	-11.86	-25.44	-6.79	5.00
2.00	22.51	21.01	20.46	7.91	21.01	28.34
2.05	-28.50	-20.46	-19.28	-50.66	-20.46	-1.57
2.10	-43.25	-43.59	-49.04	-69.07	-34.14	-16.40
2.15	-31.98	-34.58	-40.83	-66.08	-23.96	-0.23
2.20	-18.46	-23.83	-31.21	-61.27	-11.90	15.76
2.26	-2.59	-9.11	-16.70	-49.00	6.95	36.04
2.31	15.47	8.98	1.96	-34.98	24.28	52.11
2.36	31.40	25.38	19.09	-16.85	43.20	67.52
2.45	49.98	45.29	40.31	55.53	90.33	96.46

In comparison with Eurocode 1, part 4, it is possible to observe that the initial normal static pressures obtained by the FEM at the top of the silo (height 0 to 0.75 m) were higher than the standard ones. Furthermore, in relation to the increase in the wall friction coefficient and consequently a decrease in normal pressures, it is observed that the greater tendency of the pressures calculated using FEM to exceed the pressures obtained from the standard, also in the case of the wall friction coefficient  $\mu = 0.6$ .

Although the pressures in the static phase were generally lower than the discharge, it is possible to assume that the standard should increase the pressures when the wall friction coefficient is greater than 0.5. In addition, concerning the decrease in the specific weight of the stored product and consequently the decrease in normal pressures, it is observed a greater tendency of the pressures calculated through the MEF to exceed the pressures obtained from Eurocode 1, part 4, even exceeding in the case of the specific weight of the product ( $\gamma$ ) 6.0 KN m<sup>-3</sup>. Therefore, despite being pressures in the static phase, generally lower than the discharge, it is possible to assume that the standard should increase the pressures for products with lower specific weights. It can be seen that Eurocode safely increases the normal static pressures for silo projects in extreme conditions (products with

higher specific weights and lower wall friction coefficient), however, under conditions of low normal pressures the trend of pressures by FEM exceeds those of Eurocode 1, part 4.

According to Gallego (GALLEGO *et al.*, 2015) in evaluating wheat efforts experimentally, numerically, and by comparing with Eurocode 1, part 4 (CEN, 2006), pressures with magnitudes close to that of this work are found for similar properties of the stored material. Ruiz and collaborators (COUTO *et al.*, 2012), also using wheat, found that the maximum vertical pressure obtained experimentally in loading is close to the model proposed in the present work. The experimental study using corn (COUTO *et al.*, 2013) also showed a tendency for pressure values in the silo during loading close to those presented in this work.

The variation of the wall friction coefficient considerably influences the study and silo projects, changing the coefficient by only 0.4; an increase is found in the maximum normal static pressure of 58%. The same importance can be considered for the specific weight of the stored product, with an increase of 62% due to the increase in weight by 3 KN m<sup>-3</sup>. The specific weight of the stored product has an increase of 62% due to the increase in weight by 3 KN m<sup>-3</sup>.

For all the generated models, the location was

exactly 4.8 cm below the transition (both for the variation of the wall friction coefficient and the specific weight of the stored product).

## CONCLUSIONS

- The use of FEM for the calculation of pressures in silos is recommended. The two variables (specific weight and wall friction coefficient) influence the static pressures in the silo, which were observed in the pressures obtained by Eurocode and also in the results of the simulated models.
- Products with similar particular characteristics are considered. In this experiment, the highest normal static pressures will occur in the products with the highest specific weight and the lowest wall friction coefficient.
- Compared with Eurocode 1, part 4 (CEN, 2006), it could be seen that all models generated by the MEF show consistent errors, presenting normal static pressures below the standard. However, two issues were observed: although the normal pressures at the top of the silo are the lowest, the model created by the MEF presented a divergence from the standard; the second issue is related to the higher coefficient used in the standards for products that tend to have higher pressures and lower coefficients for products that tend to generate lower pressures, in other words, for products stored with lower specific weight and higher wall friction coefficient, the standard presents lower safety coefficients that could be observed in the comparisons with MEF.
- The variation of the wall friction coefficient and specific weight considerably influences the study and silo projects.
- The location of the maximum normal static pressure in the silo is located in the silo-hopper transition zone.

## ACKNOWLEDGMENTS

The authors would like to thank CAPES for financing the study and the partnership between the Federal University of Lavras and the University of

León. They are also grateful for the partnership with the University of León (Spain).

## AUTHORSHIP CONTRIBUTION STATEMENT

**GANDIA, R.M.:** Formal Analysis, Investigation, Methodology, Validation, Writing – original draft; Writing – review & editing; **GOMES, F.C.:** Conceptualization, Funding acquisition, Resources, Visualization; **DE PAULA, W.C.:** Investigation, Software, Supervision, Visualization, Writing – review & editing; **RODRIGUEZ, P.J.A.:** Data curation, Project administration, Supervision, Validation, Writing – review & editing.

## DECLARATION OF INTERESTS

The authors declare that they have no knowledge of a conflict of interest that could have appeared to influence the work reported in this paper.

## REFERENCES

- AYUGA, F.; AGUADO, P.; GALLEGO, E.; RAMIREZ, A. Experimental tests to validate numerical models in silos design. **2006 ASABE Annual International Meeting**, v. 0300, n. 06, 2006.
- BROWN, C. J.; LAHLOUH, E. H.; ROTTER, J. M. Experiments on a square planform steel silo. **Chemical Engineering Science**, v. 55, n. 20, p. 4399-4413, 2000.
- BROWN, C. J.; NIELSEN, J. **Silos: Fundamentals of theory, behaviour and design**. London: [s.n.].
- BYWALSKI, C.; KAMIŃSKI, M. A case study of the collapse of the over-chamber reinforced concrete ceiling of a meal silo. **Engineering Structures**, v. 192, p. 103-112, 2019.
- CALIL, J. C.; CHEUNG, A. B. **Silos: pressões, fluxo, recomendações para o projeto e exemplo de cálculo**. São Carlos: [s.n.].
- CEN. **EN 1991-4:2006. Eurocode 1: Actions on Structures. Part 4: Silos and Tanks**. Brussels: [s.n.].

- CONAB - Companhia Nacional de Abastecimento. **Acompanhamento da safra brasileira 2019/2020 Acompanhamento da Safra Brasileira de Grãos 2019/2020**. [s.l: s.n.]. Available in: <<https://www.conab.gov.br/info-agro/safras>>.
- COUTO, A.; RUIZ, A.; AGUADO, P.J. Measuring pressures in a slender cylindrical silo for storing maize. Filling, static state and discharge with different material flow rates and comparison with Eurocode 1 part 4. **Computers and Electronics in Agriculture**, v. 96, p. 40-56, 2013.
- COUTO, A.; RUIZ, A.; AGUADO, P. J. Design and instrumentation of a mid-size test station for measuring static and dynamic pressures in silos under different conditions - Part I: Description. **Computers and Electronics in Agriculture**, v. 85, p. 164-173, 2012.
- DIN. **DIN 1055-6: Basis of design and actions on structures – Part 6: design 623 loads for buildings and loads in silo bins**. Berlin, Verlaz: 2005.
- DOGANGUN, A.; KARACA, Z.; DURMUS, A.; SEZEN, H. Cause of damage and failures in silo structures. **Journal of Performance of Constructed Facilities**, v. 23, n. 2, p. 65-71, 2009.
- DPE - DIRETORIA DE PESQUISA E COORDENAÇÃO AGROPECUÁRIA. **IBGE - Pesquisa de Estoques 2º semestre de 2019**. [s.l: s.n.].
- DRUCKER, D. C.; PRAGER, W. Soil mechanics and plastic analysis or limit design. **Quart. Appl. Math**, v. 10, n. 2, p. 157-165, 1952.
- GALLEGO, E.; ROMBACH, G.A.; NEUMANN, F.; AYUGA, F. SIMULATIONS OF GRANULAR FLOW IN SILOS WITH DIFFERENT FINITE ELEMENT PROGRAMS: ANSYS VS. SILO. **Transactions of the ASABE**, v. 53, n. 3, p. 819-829, 2010.
- GALLEGO, E.; RUIZ, A.; AGUADO, P. J. Simulation of silo filling and discharge using ANSYS and comparison with experimental data. **Computers and Electronics in Agriculture**, v. 118, p. 281-289, 2015.
- GANDIA, R.M.; GOMES, F.C.; PAULA, W.C. DE, JUNIOR; E.A. DE O.; RODRIGUEZ, P.J.A. Static and dynamic pressure measurements of maize grain in silos under different conditions. **Biosystems Engineering**, v. 209, p. 180-199, 2021.
- GUTIÉRREZ, G.; COLONNELLO, C.; BOLTENHAGEN, P.; DARIAS, J.R.; PERALTA-FABI, R.; BRAU, F.; CLÉMENT, E. Silo collapse under granular discharge. **Physical Review Letters**, v. 114, n. 1, p. 5-9, 2015.
- HÄRTL, J.; OOI, J.Y.; ROTTER, J.M.; WOJCIK, M.; DING, S.; ENSTAD, G.G. The influence of a cone-in-cone insert on flow pattern and wall pressure in a full-scale silo. **Chemical Engineering Research and Design**, v. 86, n. 4, p. 370–378, 2008.
- HOLST, J.M.F.G.; OOI, J.Y.; ROTTER, J.M.; RONG, G.H. Numerical Modeling of Silo Filling. I: Continuum Analyses. **Journal of Engineering Mechanics**, v. 125, n. 1, p. 94-103, 1999.
- INTERNACIONAL ORGANIZATION FOR STANDARDIZATION. **ISO 11697:2012. Bases for design of structures - Loads due to bulk materials**. [s.l: s.n.].
- JANSSEN, H. A. Versuche uber getreidedruck in silozellen. **Z. Ver. Dtsch. Ing.**, v. 39, n. 35, p. 1045-1049, 1895.
- JENIKE, A. W.; JOHANSON, J. R.; CARSON, J. W. Bin loads—part 3: mass-flow bins. **Journal of Manufacturing Science and Engineering, Transactions of the ASME**, v. 95, n. 1, p. 6-12, 1973.
- MOYA, M.; AYUGA, F.; GUAITA, M.; AGUADO, P. MECHANICAL PROPERTIES OF GRANULAR AGRICULTURAL MATERIALS. **Transactions of the ASABE**, v. 45, n. 5, p. 1569-1577, 2002.
- MOYA, M.; GUAITA, M.; AGUADO, P.; AYUGA, F. MECHANICAL PROPERTIES OF GRANULAR AGRICULTURAL MATERIALS, PART 2. **Transactions of the ASABE**, v. 49, n. 1998, p. 479-490, 2006.

- NETO, J. P. L.; NASCIMENTO, J. W. B. DO; SILVA, R. C. FORÇAS DE ATRITO EM SILOS VERTICAIS DE PAREDES LISAS EM DIFERENTES RELAÇÕES ALTURA/DIÂMETRO. **Eng. Agríc., Jaboticabal**, v. 34, n. 1, p. 8-16, 2014.
- PARDIKAR, K.; ZAHID, S.; WASSGREN, C. Quantitative comparison of experimental and Mohr-Coulomb finite element method simulation flow characteristics from quasi two-dimensional flat-bottomed bins. **Powder Technology**, v. 367, p. 689-702, 2020.
- RAMÍREZ, A.; NIELSEN, J.; AYUGA, F. On the use of plate-type normal pressure cells in silos. Part 1: Calibration and evaluation. **Computers and Electronics in Agriculture**, v. 71, n. 1, p. 71-76, 2010.
- RUIZ, A.; COUTO, A.; AGUADO, P. J. Design and instrumentation of a mid-size test station for measuring static and dynamic pressures in silos under different conditions - Part II: Construction and validation. **Computers and Electronics in Agriculture**, v. 85, p. 174-187, 2012.
- SCHURICHT, T.; FURLL, C.; EENSTAD, G. G. Full scale silo tests and numerical simulations of the „cone in cone” concept for mass flow. In: **Handbook of Powder Technology**. [s.l.] Elsevier Science BV, 2001. v. 10p. 175-180.
- SCHWAB, C. V.; ROSS, I.J.; WHITE, G.M.; COLLIVER, D.G. WHEAT LOADS AND VERTICAL PRESSURE. v. 37, n. 5, p. 1613-1619, 1994.
- SUN, W.; ZHU, J.; ZHANG, X.; WANG, C.; WANG, L.; FENG, J. Multi-scale experimental study on filling and discharge of squat silos with aboveground conveying channels. **Journal of Stored Products Research**, v. 88, e101679, 2020.
- SUN, Y.; WANG, Y. Collapse reasons analysis of a large steel silo. **Advanced Materials Research**, v. 368-373, p. 647-650, 2012.
- TENG, B. J. Plastic collapse at lap joints in pressurized cylinders under axial load. **Journal of Structural Engineering**, v. 120, n. 1, p. 23-45, 1994.
- TENG, J. G.; LIN, X. Fabrication of small models of large cylinders with extensive welding for buckling experiments. **Thin-Walled Structures**, v. 43, n. 7, p. 1091-1114, 2005.
- TENG, J. G.; ROTTER, J. M. Plastic collapse of restrained steel silo hoppers. **Journal of Constructional Steel Research**, v. 14, n. 2, p. 139-158, 1989.
- TENG, J. G.; ZHAO, Y.; LAM, L. Techniques for buckling experiments on steel silo transition junctions. **Thin-Walled Structures**, v. 39, n. 8, p. 685-707, 2001.
- TENG, J.; ROTTER, J. M. Collapse Behavior and Strength of Steel Silo Transition Junctions. Part I: Collapse Mechanics. **Journal of Structural Engineering**, v. 117, n. 12, p. 3587-3604, 1991.
- WALKER, D. An approximate theory for pressures and arching in hoppers. **Chemical Engineering Science**, v. 22, n. 3, p. 486, 1967.
- WALTERS, J. K. A theoretical analysis of stresses in axially-symmetric hoppers and bunkers. **Chemical Engineering Science**, v. 28, n. 3, p. 779-789, 1973a.
- WALTERS, J. K. A theoretical analysis of stresses in silos with vertical walls. **Chemical Engineering Science**, v. 28, p. 13-21, 1973b.
- ZHAO, Q.; JOFRIET, J. C. Structural loads on bunker silo walls: Numerical study. **Journal of Agricultural Engineering Research**, v. 51, n. C, p. 1-13, 1992.
- ZHAO, Y.; TENG, J. G. Buckling experiments on steel silo transition junctions. II: Finite element modeling. **Journal of Constructional Steel Research**, v. 60, n. 12, p. 1803-1823, 2004.
- ZHONG, Z.; OOI, J. Y.; ROTTER, J. M. The sensitivity of silo flow and wall stresses to filling method. **Engineering Structures**, v. 23, n. 7, p. 756-767, 2001.